Enhanced power generation from the interaction between sweat and electrodes for human health monitoring

Heting Wu[†,‡], Lin Xu[†,⊥], Yang Wang[†], Tongtong Zhang[†,‡], Hainan Zhang[†], Chris R. Bowen[§], Zhong Lin Wang[†,∥,], and Ya Yang[†,‡,⊥,]**

[†]CAS Center for Excellence in Nanoscience, Beijing Key Laboratory of Micro-nano Energy and Sensor, Beijing Institute of Nanoenergy and Nanosystems, Chinese Academy of Sciences, Beijing 100083, P. R. China. E-mail: yayang@binn.cas.cn (Y. Yang)
[‡]School of Nanoscience and Technology, University of Chinese Academy of Sciences, Beijing, 100049, P. R. China.
[§]Department of Mechanical Engineering, University of Bath, BA27AK, UK
[∥]School of Material Science and Engineering, Georgia Institute of Technology, Atlanta, GA 30332-0245, USA. E-mail: zhong.wang@mse.gatech.edu (Z. L. Wang)
[⊥]Center on Nanoenergy Research, School of Physical Science and Technology, Guangxi University, Nanning 530004, PR China.
*To whom correspondence should be addressed: Email: yayang@binn.cas.cn (Y. Yang), zhong.wang@mse.gatech.edu (Z. L. Wang).

ABSTRACT: Power generation from human sweat has attracted great attention due to its potential application in waste energy scavenging. However, the development of methods to generate sufficient electricity from sweat to power electronic devices for health monitoring remains a major challenge. Here, we report a wearable sweat-based electricity generator (SEG), in which the power generation mechanism is based on redox reaction between sweat and electrodes. Due to the increase in oxygen adsorption, both the output current and power of SEG with single-walled carbon nanotubes modified electrode can be remarkably enhanced by 5.6 and 14.7 times compared to SEG with nanotubes-free electrode, respectively. The SEGs have been first utilized to power a wireless heart-rate sensor for sustainably transmitting heart-rate data to a smart-phone. Moreover, self-powered sensing of lactic acid has been achieved by electric signals with the current sensitivity of 11.79 $mmol \cdot L^{-1} \cdot mA^{-1}$, demonstrating applications in human health care.

Recently, collecting energy from waste produced by human activities has become a topic of academic and industrial interest.[1-8] The pervasiveness of human sweat has attracted growing interest in the development of sweat-based energy harvesting technologies. Sweat possesses abundant resources for energy generation since it contains solutes of lactic acid, glucose, urea, and minerals. With the increasing adoption of portable and wearable electronic devices, a wearable sweat-based electricity generator (SEG) has significant potential to act as an alternative power source to batteries.[9] Currently, SEGs are based on smart tattoos,[8,10,11] a micro-wearable device that contains integrated circuits and communication functions. Although this approach may have potential to power wearable devices, the most significant challenge is that their power level is relatively low. Another type of SEG is the fuel cell based sweat sensors.[12-20] These biofuel cells are powered by lactic acid in sweat, and the lactic acid can be used to create miniature fuel cells.[13,14] As an example, a sweat wristband, fabricated by connecting 4 photocatalytic biofuel cells in series, generated a voltage of 0.94 V and a current of 0.35 mA, leading to a relatively low power of 0.328 mW.[14] There is still a requirement to use additional batteries with the lactic acid sensor to store electricity. Moreover, the low stability of power generated by the cells cannot ensure successful operation of electronic equipment.[2,15-24] While tattoos and biofuel cells can provide mechanical flexibility to a wearable SEG devices, this device architecture has difficulties in gathering sufficient human sweat to convert into electricity.[25-29]

Currently, scientists are seeking to amplify the electric power produced by biofuel cells to drive larger portable electronic devices, including heart rate sensors, smart watches, smart phones, etc.[12-20] A stretchable device has recently been developed to generate electricity by altering the chemical compounds in sweat. It was able to generate electricity by oxidizing the lactic acid in sweat, leading to a maximum output power of 0.45 mW.[13] However, it can only power a single light-emitting diode in two modes, continuous discharge, and pulse discharge, it cannot provide sufficient power for a larger portable electronic device. Therefore, the key challenge for the effective application of wearable SEGs is to create a device that is able to simultaneously meet the following requirements: 1) Provide a new electricity generation mechanism to realize a larger output current for directly

powering human health monitoring-related devices; 2) Enable self-powered sensing of lactic acid level by the analysis of human sweat; 3) Flexible and wearable characteristics for the convenient integration of wearable devices on human body.

Here we have designed a new type of SEG with an interdigitative electrode structure that exploits a redox reaction, where the interaction between the electrodes and sweat (human sweat as the electrolyte) can generate electric power. A carbon nanotube coating, that is formed by physical deposition on the surface of copper foil cathode, has been found to improve the oxygen absorption capacity and electron transfer rate, resulting in an optimized SEG that can deliver an output voltage of 0.81 V, a record-breaking current of 16.58 mA, and a maximum power of 2.2 mW, where both the output current and power are much higher than any other SEG reported to date (Table S1). The fabricated SEGs have been utilized to generate sufficient electric energy from human sweat to directly power a wireless heart rate sensor and continuously transmit exercise heart rate data to a cell phone, which is of great significance to human health monitoring. Moreover, we measured the performance of the SEGs using sweat samples from 34 different people and conducted a mathematical statistical analysis on their lactic acid content, output current, and other relevant data. By analysis of these data, it was possible to realize self-powered sensing of lactic acid with a current sensitivity of 11.79 $mmol \cdot L^{-1} \cdot mA^{-1}$, which breaks the traditional battery-powered sensor paradigm. The fabricated SEGs can enable the monitoring of human exercise heart rate and sweat lactic acid level, exhibiting potential applications in the human health care field.

Based on redox-induced electricity,[29-32] the cathode and anode of the SEG can react electrochemically with sweat to produce an electrical output, which can directly power a wireless heart rate belt to provide the function of self-powered real-time heart rate monitoring. Moreover, the lactic acid level of the sweat has a linear relationship with the current signal of the SEG, so that the

device has a higher current response and a larger detection range at higher lactic acid levels. We found that different people have different levels of lactic acid in their sweat and since the electrical output increases with the lactic acid level in sweat, the output current of the SEG can be used to determine the lactic acid level of sweat for each person. The device is simple to fabricate (Supplemental Note 1) and provides a larger output current than existing sweat generators, which can effectively exploit human sweat to generate electricity. The power levels are sufficiently large and stable to power wireless heart rate sensors and can realize the detection of the lactic acid level of human sweat, which has potential applications, as illustrated Figure 1a (Movie S1).

For the electricity generation mechanism, the reduction reaction ($O_2 + 2H_2O + 4e^- \rightarrow 4OH^-$) occurs at the CNT coated copper foil cathode, while the oxidation reaction ($Zn - 2e^- \rightarrow Zn^{2+}$) occurs at the zinc anode, as displayed in Fig. 1b. Spontaneous oxygen reduction reactions (ORR) at the interfaces between the sweat and the electrodes allow the large number of electrons to flow through the external circuit (Fig. 1b), inducing a constant DC output current. The direction of current is opposite to the direction of electrons (from Zn to Cu), the direction of current is from Cu cathode to Zn anode. From the equations of the reaction above, it can be seen that the ability to obtain sufficient oxygen from the cathode materials can determine the output performance of the device. Moreover, the output performance is associated with the difference between the cathode and anode materials, where we choose the Cu and Zn films, respectively, with the purpose of a creating a low cost device based on materials that are abundantly available.

For these purposes, we designed a SEG consisting of a Zn film anode and a CNT coated Cu film as the cathode, where the CNTs can effectively enhance the capacity of obtaining oxygen due to the high surface area nanotube structure, as illustrated in Figure 1c. Figure 1d displays a photograph of the designed SEG with a length of ~ 9.3 cm and a width of ~ 4 cm (Supplemental Note 2), which

exhibits both wearable and flexible features, as depicted in Figure 1e. Careful inspection of the role and influence of the carbon nanotube[33,34] coating demonstrates that it acts to increase the specific surface area of the cathode and its ability to absorb oxygen (Figure 1c).

We explore how to optimize the output performance of the SEG device. It is worth noting that sweat samples used in the following experiments are achieved using commercial synthetic perspiration. The device design and optimization considered the following key aspects: the selection of the cathode carbon coating material (Figure 2a), the distribution of the number of cathode and anode fingers in the interdigitated cross finger electrode structure of the SEG (Figure S2a,b), the volume of cathode coated carbon nanotubes in the water dispersion (Figure S3a) and the thickness of cathode copper foil (Figure S3b). Due to the limitations of the sophisticated surface structure of human skin, the design of the device should not only consider the area of the device, but also pay more attention to its practical application significance. Our design is based on realizing self-powered human health management, so improving the absolute output power, voltage, and current of the equipment is our design focus. To determine the degree of correlation between the measured variables and output current a *grey system theory* model was used.[35] As seen in Figure S3c, the calculated grey correlation between all variables and the output current of the SEG is greater than 0.5, which indicate that all variables contribute to the output current. From the above design and optimization process, we manufactured an optimized SEG device, as displayed in Figure 1d,e.

We compared the impact of different carbon nanotube coatings on the output performance of the SEG. We characterized single-walled carbon nanotubes (SWCNT) and multi-walled carbon nanotubes (MWCNT) as typical nanotube sources and assessed SEG devices without any carbon nanotubes as a control reference. Noticeable differences between the SWCNT and MWCNT are highlighted both in the scanning electron microscope (SEM) observations in Figure 4a-d and atomic

force microscopy (AFM) analysis of individual carbon nanotubes in Figure 2b,c. A detailed description of their morphology can be seen in Supplemental Note 3.

The most striking observation to emerge from the data comparison was that the record-breaking output current of the cathode-coated SWCNT generator is approximately twice as high as that of a cathode-coated MWCNT generator (Figure 2d). Figure 2e presents the output current and power of the SEG results obtained from the initial measurement of three separate SEGs with (i) a nanotube-free copper foil cathode, (ii) a MWCNT coated copper foil cathode and (iii) a SWCNT coated copper foil cathode. On comparing each device, the nanotube-free SEG with no coating has the lowest output current (2.98 mA) and power (0.15 mW). On modifying the copper foil surface with MWCNTs, the output current and power is increased by 2.8 times and 11.3 times to 8.25 mA and 1.8 mW. For the SEG with a copper foil cathode coated with the smaller diameter SWCNTs (the average outer diameter of SWCNT is ~ 30 nm, and that of MWCNTs is ~ 100 nm, as shown in Figure S4) the output current and power increased to an even greater extent by 5.6 times and 14.7 times to 16.58 mA and 2.2 mW, respectively (Table S2 and Supplemental Note 4). Both the obtained output current and power represent the highest reported values when compared all other reported sweat generator data (Table S1). Moreover, the sweat generating devices coated with SWCNT have favorable electrical signal cycling stability and mechanical stability, see Figure S6d-f.

After the series of optimization processes the optimum sweat power generation device was manufactured, which consisted of a cathode electrode layer and a anode electrode layer to form a planar micro-pitch interdigitated electrode structure (Supplemental Note 2). The output voltage of this device is 0.81 V (Figure S5a), with a record-breaking current of 16.58 mA (Figure S5b), and maximum power of 2.2 mW (Figure S6c). The output voltage (Figure 2f), current (Figure 2g) and power (Figure 2h) of the SEG is much better than similar battery-free sweat-based electronic devices

and provides new opportunities for driving wearable electronic devices with larger power requirements[36,37].

The physical and chemical adsorption capacity of the SWCNTs and MWCNTs were further compared to study the mechanism by which the CNTs coated on the cathode enhanced the output current of the SEG. The following is a brief description of the power enhancement mechanism: due to their smaller diameter, the SWCNTs have a larger specific surface area and a greater ability to absorb oxygen chemically than MWCNTs, therefore it is likely that the effect of the coating is to increase the specific surface area of the cathode and its capacity to absorb oxygen. In addition, the SEG coated with SWCNTs (see Supplemental Note 5) has outstanding electrochemical properties in terms of higher output current signals. As a result, there is an increase in the rate of electrochemical reaction and electron transfer, and an increase in the current generated by the SEG (Figure 3a and Supplemental Note 6). Figure 3b demonstrates the BET surface area plot of SWCNTs and MWCNTs, from which we can determine that their BET specific surface area as 194.1020 m^2/g and 94.6514 m^2/g respectively, the data is further displayed in the blue column of Figure 3e. These results summarize the surface area, pore size and pore volume of SWCNTs and MWCNTs samples, estimated by the adsorption-desorption measurement of BET (Brunauer Emmett Teller). The data obtained confirm that the SWCNT has a greater porosity volume than MWCNT (Figure S7c and Supplemental Note 7), and therefore the SWCNT has a larger specific surface area for high electrical activity.

According to Figure 3c, through a comparison with MWCNT, the smaller active particle diameter (hemisphere 3.0878 nm) and cubic crystallite size (2.5732 nm) of the SWCNT deposited on the cathode can provide a high ORR activity for the SEG. Pulse chemisorption analysis data, shown in Figure 3d, indicate that in 140 min, the cumulative quantity of oxygen adsorbed by SWCNT and

MWCNT is 0.42140 cm^3/g STP and 0.05647 cm^3/g STP respectively, and the data is also shown by the red column of Figure 3e. In essence, the BET specific surface area and the cumulative quantity of oxygen adsorbed by SWCNTs are considerably higher than those of MWCNTs. Moreover, the SWCNTs have a smaller active particle diameter (Figure S7b) and crystallite size, that provides increased active area. These advantages lead to the electrochemical reaction of the SWCNT reformative of the SEG cathode being more efficient and producing a greater output current.

Carbon nanotubes therefore play an important role in improving the output current performance of SEG. Carbon nanotubes exhibit the chaacteristics of small diameter and large length-to-diameter ratio. They are highly suitable for constructing a lightweight and excellent conductive network without hindering ion transmission, which is highly conducive to our fabrication of a SEG based on electrochemical principles.

The primary purpose of the current study is to identify the ability to use human waste sweat to generate electricity for powering electronic devices. As highlighted in the previous section, the output voltage/current of a single SEG device is approximately 0.81 V/16.58 mA. Due to the high current output characteristics of SEGs, simply connecting a plurality of SEG devices in series can power and function electronic devices such as LEDs (Figure 4a,b) and heart rate bands (Figure 4c,d). As illustrated in Figure S9a, four SEGs are connected in series for integration into a wearable sweat-absorbent headband with 11 N-shaped LED lights attached. After an athlete or fitness enthusiast puts on the integrated headband and begins a sporting activity, such as running, sweat is generated. As the exercise process proceeds, the runner will usually secrete sweat after approximately 15 minutes. The four SEGs absorb sufficient sweat and, when connected to the N-shaped lights on the headband, can illuminate them (Figure 4a,b, Movie S2). This feature is useful for sports enthusiasts who like to run in the evening or at night. Similar to the headband, 12 SEGs in

series (Figure S9b) were connected to an integrated wireless Bluetooth wearable heart rate band (Figure 4c,d). After approximately 30 minutes of continuous exercise, all 12 SEGs located on the back of the runner also had an abundant level of sweat, which were connected to the heart rate belt. The voltage and current provided by the SEGs connected in series successfully allowed the heart rate monitoring belt to operate steadily. The heart rate data were monitored and transmitted to the smart phone for continuous monitoring of exercise heart rate (Figure 4e,f) (Movie S3). SEG can directly provide a stable power supply for the heart rate belt for its operation. In this circuit, no power conversion and management is required.

The fabricated wearable device represents an integrated self-powered system. Depending on the SWCNTs coating of the cathode, the output current of SEG is raised to levels of approximately 16.6 mA. In real-life scenarios, the long-term stability and flexibility of the SEG render it suitable for many types of wearable electronics, especially heart rate sensors. Although the anode zinc foil in the SEG is consumed due to redox reaction, this process is slow over the entire course of the reaction. A SEG-driven wireless heart rate belt has been realized, as illustrated in Figure 4d,f. The heart rate is, in fact, the best exercise "instructor", and we can better control exercise intensity based on heart rate data, since the heart rate is linearly associated with oxygen intake and maximum oxygen uptake, and the percentage of maximum heart rate is also proportional to the percentage of maximum oxygen uptake. The relationship is rectilinear, and the ability to continuously monitoring heart rate allows people to know how to maintain a heart rate range in real-time when running or undertaking aerobic exercises.

To perform an exploratory study using the optimized SEGs, 34 subjects were used in this work, and human sweat produced during bodily exercise was collected with informed consent. In detail, we not only collected sweat samples of approximately 5 mL per subject (Figure S10a) but also

statistically recorded anthropometric data such as age, gender, pH of sweat and body mass index (BMI). Next, we measured the output current (Figure 5a) and voltage (Figure S11a) of all 34 sweat samples generated by their respective SEGs (Figure S10b). One of the most interesting observations was that the power output of the SEGs in different people's sweat samples exhibit different characteristics.

To understand the cause of this phenomenon, we undertook analysis of the lactic acid content in 34 sweat samples (Figure 5b) using conventional enzyme-linked immunosorbent assay (ELISA) methods. We hypothesized that the lactic acid content and the pH value of sweat samples affects the electrical output of the SEGs. For this purpose, the corresponding graphs showing the different output currents and voltages using a two-dimensional rainbow color-filled contour plot, as shown in Figure 5c,d. From the contour plot map graphs, we can observe the color sequence distribution (red, orange, yellow, green, cyan, blue, purple) of the rainbow, and we can conclude that the pH value and lactic acid content of sweat have almost no influence on the output voltage of the SEG, but they are strongly related to the output current of the SEG. In particular, the content of lactic acid in the sweat sample had the greatest influence on the output current since the distribution of the current levels from large to small lactic acid contents is virtually in the same order of the rainbow from red to purple. Then, we evaluated the correlation (Supplemental Note 8) between the SEG output current and anthropometric data including age, pH of sweat, BMI and the content of lactic acid with a Pearson correlation coefficient.[38] Based upon the results in Figure 5e, the four Pearson correlation coefficients calculated indicate that the correlation between the lactic acid content of the sweat samples and the output current of the SEG is 0.945, showing a highly significant positive correlation ($p < 0.001$, ***). The Pearson correlation coefficients between sweat pH, the age of sweat donors and the output current were -0.340 and -0.355, respectively, showing significant negative correlation

($p < 0.05$, *). The Pearson correlation coefficient between sweat donor BMI and output current is 0.010; the related degree is not clear, at least not a linear correlation ($p >> 0.1$).

A more detailed analysis of the lactic acid content of sweat and the output current of the SEGs indicates there is an excellent positive linear correlation. To determine the sensitivity of the SEG for lactic acid detection, from data fitting it was found that the linear correlation coefficient was 0.945, where the linear equation was $y = 11.79x - 13.21$ (where, x represents the output current and y represents the concentration of lactic acid in sweat). As illustrated in Figure 5f, samples with a higher output current signals of SEG also had higher lactic acid content. The SEG is therefore able to monitor the lactic acid level in human sweat by detecting the change of the current, and the sensitivity is 11.79 $mmol \cdot L^{-1} \cdot mA^{-1}$, so as to realize human health monitoring. Moreover, through careful analysis of the front and side of silhouette photos and personal information of all 34 subjects, we found that individuals with high lactic acid content in sweat are usually young (Figure S14b), fit, and are actively involved in sports and fitness, and often do yoga and other sports activities, as included in the photograph of the silhouette of the subjects inserted in the histogram of Figure 5a. In contrast, people with low sweat lactate levels, that is, low SEG output currents, are mostly elderly (Figure S14b), lean, high body mass index, or sedentary people with poor metabolic capacity[39], as provided in the photograph of the silhouette of the subjects inserted in the histogram of Figure 5b.

These experiments confirmed that the lactic acid content in the sweat sample and the output current of its SEG exhibits a highly significant and linear relationship so that the SEG also has the ability to detect lactic acid levels, the possible mechanism is described in Supplemental Note 9. Moreover, during strenuous exercise, the metabolism of muscle cells will be converted into a lactic acid fermentation process (Supplemental Note 10). During this process, lactic acid begins to accumulate in the muscles and subsequently discharges through sweat. If the lactic acid level

increases above a specific threshold, this can result in both muscle fatigue and dehydration. Therefore, it is desirable that a wearable sweat power generation device is also able to continuously monitor lactic acid levels in sweat. The concentration of lactic acid in human sweat is due to the body's metabolism and level of exertion since the intermediate products produced during the metabolism of glucose in the human body (mainly in muscle cells) are mainly lactic acid (Figure S14a). Continuous aerobic exercise promotes the acceleration of energy metabolism and encourages lactic acid to be excreted in sweat. The level of lactic acid in human sweat can also reflect the metabolic level of the human body to a certain extent, which is consistent with our research results (Figure S14b, Supplemental Note 11).

In most wearable devices, batteries are currently used to provide a sufficient power source. Whether they are rechargeable lithium-ion batteries or disposable alkali-generated batteries, these ubiquitous battery-based devices face many issues such as a need for periodic charging, low portability and low energy density. There is therefore growing interest in creating wearable energy scavenging devices. We have developed a novel strategy to extract energy from the interaction between sweat and electrodes. Through the optimized design of the SWCNTs-modified electrode, the output current of the SEG can be significantly improved for providing an improved ability to absorb oxygen and enhance the electron transfer rate. As a result, the SWCNTs-modified device can deliver an output current of 16.58 mA, leading to a power level of 2.2 mW. This power level is suitable for a variety of potential applications, in particular wearable electronic devices such as wireless heart rate monitoring belts that can be directly powered using the SEGs to obtain electric energy from sweat.

A significant finding to emerge from this study is that SEG is not only a electricity generator with high current and power output, but it also has the multi-functional ability to monitor the lactic

acid level of sweat. This work provides a new method of energy scavenging from human sweat for directly driving wireless heart rate sensors and self-powered sensing of human sweat lactic acid level, which could push human sweat related energy harvesters and health monitoring sensors to a new stage.

ASSOCIATED CONTENT

Supporting Information

The Supporting Information is available free of charge on the ACS Publications website.

Schematic of the fabrication process for the SEG and optical image of SEGs.Schematic of the fabrication process for the SEG and optical image of SEGs.; Schematic of optimization of the number of cathode and anode interdigital electrodes of a SEG.; Optimal design of cathode carbon nanotube coating and cathode copper foil thickness for a SEG.; Characterization of SWCNTs and MWCNTs.; Measurement of output voltage and output current of SEGs.; Current-power curve diagram of SEGs and output performance and stability test chart of optimal device.; The electrochemical characteristics of SEGs and the adsorption results of carbon nanotubes.; Characterization of copper foil after electrochemical reaction with sweat.; Self-powered SEG for human health monitoring applications.; Photographs of human sweat samples and image showing sweat generating devices for testing different sweat samples.; Measured voltage of all 34 sweat samples generated by their respective SEGs, calculated grey absolute correlation degree of the sweat donor's gender, age, BMI value, sweat pH value and the output current, and output voltage of the SEGs respectively.; Information of 18 male subjects' silhouette photos.; Information of 16 female subjects' silhouette photos.; Statistical analysis of human sweat with SEGs.; 3D Color-mapping

surface plot of the sweat donors' gender, age, BMI, sweat pH, sweat lactic acid content and the output performance of each SEG. (PDF)

AUTHOR INFORMATION

Corresponding Author

*Email: yayang@binn.cas.cn, zhong.wang@mse.gatech.edu.

Notes

The authors declare no competing financial interest.

ACKNOWLEDGMENTS

This work was supported by the National Key R&D Project from Minister of Science and Technology in China (No. 2016YFA0202701), the University of Chinese Academy of Sciences (Grant No. Y8540XX2D2), the National Natural Science Foundation of China (No. 51472055), External Cooperation Program of BIC, Chinese Academy of Sciences (No. 121411KYS820150028), the 2015 Annual Beijing Talents Fund (No. 2015000021223ZK32), and Qingdao National Laboratory for Marine Science and Technology (No. 2017ASKJ01).

REFERENCES

（1）Mishra, A. K; Wallin, T. J.; Pan, W.; Xu, P.; Wang, K.; Giannelis, E. P.; Mazzolai, B.; Shepherd, R. F. Autonomic perspiration in 3D-printed hydrogel actuators. *Sci. Robot.* **2020***, 5*, eaaz3918.

（2）Guan, H.; Zhong, T.; He, H.; Zhao, T.; Xing, L.; Zhang, Y.; Xue, X. A self-powered wearable sweat-evaporation-biosensing analyzer for building sports big data. *Nano Energy* **2019**, *59*, 754-761.

（3）Kim, J.; Campbell, A. S.; de Avila, B. E.; Wang, J. Wearable biosensors for healthcare monitoring. *Nat. Biotechnol*. **2019**, *37*, 389-406.

（4）Kishore, R. A.; Nozariasbmarz, A.; Poudel, B.; Sanghadasa, M.; Priya, S. Ultra-high performance wearable thermoelectric coolers with less materials. *Nat. Commun.* **2019**, *10*, 1765.

（5）Aubin, R. A.; Choudhury, S.; Jerch, R.; Archer, L. A.; Pikul, J. H.; Shepherd, R. F. Electrolytic vascular systems for energy-dense robots. *Nature* **2019**, *571*, 51-57.

（6）Liu, X.; Gao, X.; Ward, J. R.; Liu, X.; Yin, B.; Fu, T.; Chen, T.; Lovley, D. R.; Yao, J. Power generation from ambient humidity using protein nanowires. *Nature* **2020**, *578*, 550-554.

（7）Seshadri, D. R.; Li, D. R.; Voos, J. E.; Rowbottom, J. R.; Alfes, C. M.; Zorman, C. A.; Drummond, C. K. Wearable sensors for monitoring the physiological and biochemical profile of the athlete. *NPJ Digit. Med.* **2019**, *2*, 72.

（8）Reeder, J. T.; Choi, J.; Xue, Y.; Gutruf, Y.; Hanson, Y.; Liu, M.; Ray, T.; Bandodkar, A. J.; Avila, R.; Xia, W.; Krishnan, S.; Xu, S.; Barnes, K.; Pahnke, M.; Ghaffari, R.; Huang, Y.; Rogers, J. A. Waterproof, electronics-enabled, epidermal microfluidic devices for sweat collection, biomarker analysis, and thermography in aquatic settings. *Sci. Adv.* **2019**, *5*, eaau6356.

（9）Currano, L. J.; Sage, F. C.; Hagedon, M.; Hamilton, L.; Patrone, J.; Gerasopoulos, K. Wearable sensor system for detection of lactate in sweat. *Sci. Rep.* **2018**, *8*, 15890.

（10）Koh, K.; Kang, D.; Xue, Y.; Lee, S.; Pielak, R. M.; Kim, J.; Hwang, T.; Min, S.; Banks, A.; Bastien, P.; Manco, M. C.; Wang, L.; Ammann, K. R.; Jang, K. I.; Won, P.; Han, S.; Ghaffari, R.; Paik, U.; Slepian, M. J.; Balooch, G.; Huang, Y.; Rogers, M. J. A soft, wearable microfluidic device for the capture, storage, and colorimetric sensing of sweat. *Sci. Transl. Med.* **2016***, 8*, 366ra165.

（11）Chen, Y.; Lu, S.; Zhang, S.; Li, Y.; Qu, Z.; Chen, Y.; Lu, B.; Wang, X.; Feng, X. Skin-like biosensor system via electrochemical channels for noninvasive blood glucose monitoring. *Sci. Adv.* **2017***, 3*, e1701629.

（12）Pang, S.; Gao, Y.; Choi, S. Flexible and stretchable biobatteries: monolithic integration of membrane-free microbial fuel cells in a single textile layer. *Adv. Energy Mater.* **2018***, 8*, 1702261.

（13）Chen, X.; Yin, L.; Lv, J.; Gross, A. J.; Le, M.; Gutierrez, N. J.; Li, Y.; Jeerapan, I.; Giroud, F.; Berezovska, A.; O'Reilly, R. K.; Xu, S.; Cosnier, S.; Wang, J. Stretchable and flexible buckypaper-based lactate biofuel cell for wearable electronics. *Adv. Funct. Mater.* **2019**, *9*, 1905785.

（14）Lui, G.; Jiang, G.; Lenos, J.; Lin, E.; Fowler, M.; Yu, A.; Chen, Z. Advanced biowaste-based flexible photocatalytic fuel cell as a green wearable power generator. *Adv. Mater. Technol.* **2017**, *2*, 1600191.

（15）Yu, Y.; Nassar, J.; Xu, C.; Min, J.; Yang, Y.; Dai, A.; Doshi, R.; Huang, A.; Song, Y.; Gehlhar, R.; Ames, A. D.; Gao, W. Biofuel-powered soft electronic skin with multiplexed and wireless sensing for human-machine interfaces. *Sci. Robot.* **2020**, *5*, 41.

（16）Jia, W.; Valdes-Ramirez, G.; Bandodkar, A. J.;Windmiller, J. R.;Wang, J. Epidermal biofuel cells: Energy harvesting from human perspiration. *Angew. Chem. Int. Ed.* **2013**, *52*, 7233-7236.

（17）Gong, S.; Schwalb, W.; Wang, Y.; Chen, Y.; Tang, Y.; Si, J.; Shirinzadeh, B.; Cheng, W. A wearable and highly sensitive pressure sensor with ultrathin gold nanowires. *Nat. Commun.* **2014**, *5*, 3132-3140.

（18）Falk, M.; Pankratov, D.; Lindh, L.; Arnebrant, T.; Shleev, S. Miniature direct electron transfer based enzymatic fuel cell operating in human sweat and saliva. *Fuel Cells* **2014**, *14*, 1050-1056.

（19）Lee, H.; Choi, T. K.; Lee, Y. B.; Cho, H. R.; Ghaffari, R. D.; Wang, L. E.; Choi, H. J.; Chung, T. D.; Lu, N.; Hyeon, T.; Choi, S. H.; Kim, D. H. A graphene-based electrochemical device with thermoresponsive microneedles for diabetes monitoring and therapy. *Nat. Nanotechnol.* **2016**, *11*, 566-572.

（20）Bandodkar, A. J.; You, J. M.; Kim, N. H.; Gu, Y.; Kumar, R.; Mohan, A. M. V.; Kurniawan, J.; Imani, S.; Nakagawa, T.; Parish, B.; Parthasarathy, M.; Mercier, P. P.; Xu, S.; Wang, J. Soft,

stretchable, high power density electronic skin-based biofuel cells for scavenging energy from human sweat. *Energ. Environ. Sci.* **2017**, *10*, 1581-1589.

（21）Gao, W.; Emaminejad, S.; Nyein, H. Y. Y.; Challa, S.; Chen, K.; Peck, A.; Fahad, H. M.; Ota, H.; Shiraki, H.; Kiriya, D.; Lien, D. H.; Brooks, G. A.; Davis, R. W.; Javey, A. Fully integrated wearable sensor arrays for multiplexed in situ perspiration analysis. *Nature* **2016**, *529*, 509-514.

（22）Lin, R.; Kim, H. J.; Achavananthadith, S.; Kurt, S. A.; Tan, S. C. C.; Yao, H.; Tee, B. C. K.; Lee, J. K. W.; Ho, J. S. Wireless battery-free body sensor networks using near-field-enabled clothing. *Nat. Commun.* **2020**, *11*, 444.

（23）Sun, T.; Zhou, B.; Zheng, Q.; Wang, L.; Jiang, W.; Snyder, G. J. Stretchable fabric generates electric power from woven thermoelectric fibers. *Nat. Commun.* **2020**, *11*, 572.

（24）Gao, Z.; Sann, E.; Lou, X.; Liu, R.; Dai, J.; Zuo, X.; Xia, F.; Jiang, L. Naked-eye point-of-care testing platform based on a pH-responsive superwetting surface: toward the non-invasive detection of glucose. *NPG Asia Materials* **2018**, *10*, 177-189.

（25）Ortega, L.; Llorella, A.; Esquivel, J. P.; Sabate, N. Self-powered smart patch for sweat conductivity monitoring. *Microsyst. Nanoeng.* **2019***, 5*, 3.

（26）Bandodkar, A. J.; Gutruf, P.; Choi, J.; Lee, K.; Sekine, Y.; Reeder, J. T.; Jeang, W. J.; Aranyosi, W. J.; Lee, S. P.; Model, J. B.; Ghaffari, R.; Su, C. J.; Leshock, J. P.; Ray, T.; Verrillo, A.; Thomas, K.; Krishnamurthi, V.; Han, S.; Kim, J.; Krishnan, S.; Hang, T.; Rogers, J. A. Battery-free, skin-interfaced microfluidic/electronic systems for simultaneous electrochemical, colorimetric, and volumetric analysis of sweat. *Sci. Adv.* **2019***, 5*, eaav3294.

（27）Lee, H.; Song, C.; Hong, Y. S.; Kim, Y. S.; Cho, H. R.; Kang, T.; Shin, K.; Choi, S. H.; Hyeon, T.; Kim, D. H. Wearable/disposable sweat-based glucose monitoring device with multistage transdermal drug delivery module. *Sci. Adv.* **2017,** *3*, e1601314.

(28) Nyein, H. Y. Y.; Bariya, M.; Kivimaki, L.; Uusitalo, S.; Liaw, T. S.; Jansson, E.; Ahn, T. S.; Hangasky, J. A.; Zhao, J.; Lin, Y.; Happonen, T.; Chao, M.; Liedert, C.; Zhao, Y.; Tai, L. C.; Hiltunen, J.; Javey, A. Regional and correlative sweat analysis using high-throughput microfluidic sensing patches toward decoding sweat. *Sci. Adv.* **2019,** *5*, eaaw9906.

(29) Parlak, O.; Keene, L. C.; Marais, A.; Curto, V. F.; Salleo, A. Molecularly selective nanoporous membrane-based wearable organic electrochemical device for noninvasive cortisol sensing. *Sci. Adv.* **2018,** *4*, eaar2904.

(30) Wang, Y. M.; Wang, Y.; Yang, Y. Graphene-polymer nanocomposite-based redox-induced electricity for flexible self-powered strain sensors. *Adv. Ene. Mat.* **2018**, *8*, 1800961.

(31) Wang, Y.; Jiang, Y. T.; Wu, H. T.; Yang, Y. Floating robotic insects to obtain electric energy from water surface for realizing some self-powered functions. *Nano Energy* **2019**, *63*, 103810.

(32) Wang, Y.; Yang, Y. Superhydrophobic surfaces-based redox-induced electricity from water droplets for self-powered wearable electronics. *Nano Energy* **2019***, 56*, 547-554.

(33) Wang, H.; Li, P.; Yu, D.; Zhang, Y.; Wang, Z.; Liu, C.; Qiu, H.; Liu, Z.; Ren, J.; Qu, X. Unraveling the Enzymatic Activity of Oxygenated Carbon Nanotubes and Their Application in the Treatment of Bacterial Infections. *Nano Lett.* **2018**, *18*, 3344-3351.

(34) Lei, W. X.; Pan, Y.; Zhou, Y. C.; Zhou, W.; Peng, M. L.; Ma, Z. S. CNT-Cu composite layer enhanced Sn-Cu alloy as high performance anode materials for lithium-ion batteries. *RSC Adv.* **2014**, *4*, 3233-3237.

(35) Kuo, Y.; Yang, T.; Huang, G. W. The use of grey relational analysis in solving multiple attribute decision-making problems. *Comput. Ind. Eng.* **2008**, *55*, 80-93.

（36）Yang, Y.; Song, Y.; Bo, X.; Min, J.; Pak, O. S.; Zhu, L.; Wang, M.; Tu, J. A.; Kogan, H.; Zhang, T.; Hsiai, K.; Li, Z.; Gao, W. A laser-engraved wearable sensor for sensitive detection of uric acid and tyrosine in sweat. *Nat. Biotechnol.* **2020***, 38*, 217-224.

（37）Choi, J.; Ghaffari, R.; Baker, L. B.; Rogers, J. A. Skin-interfaced systems for sweat collection and analytics. *Sci. Adv.* **2018**, *4*, eaar3921.

（38）Ahlgren, P.; Jarneving, B.; Rousseau, R. Requirements for a cocitation similarity measure, with special reference to Pearson's correlation coefficient. *JASIS **2003***, *54*, 550-560.

（39）Jiang, Y.; Wang, Y.; Wu, H.; Wang, Y.; Zhang, R.; Olin, H.; Yang, Y. Laser-etched stretchable graphene–polymer composite array for sensitive strain and viscosity sensors. *Nano-Micro Letters.* **2019***, 11,* 99.

FIGURES

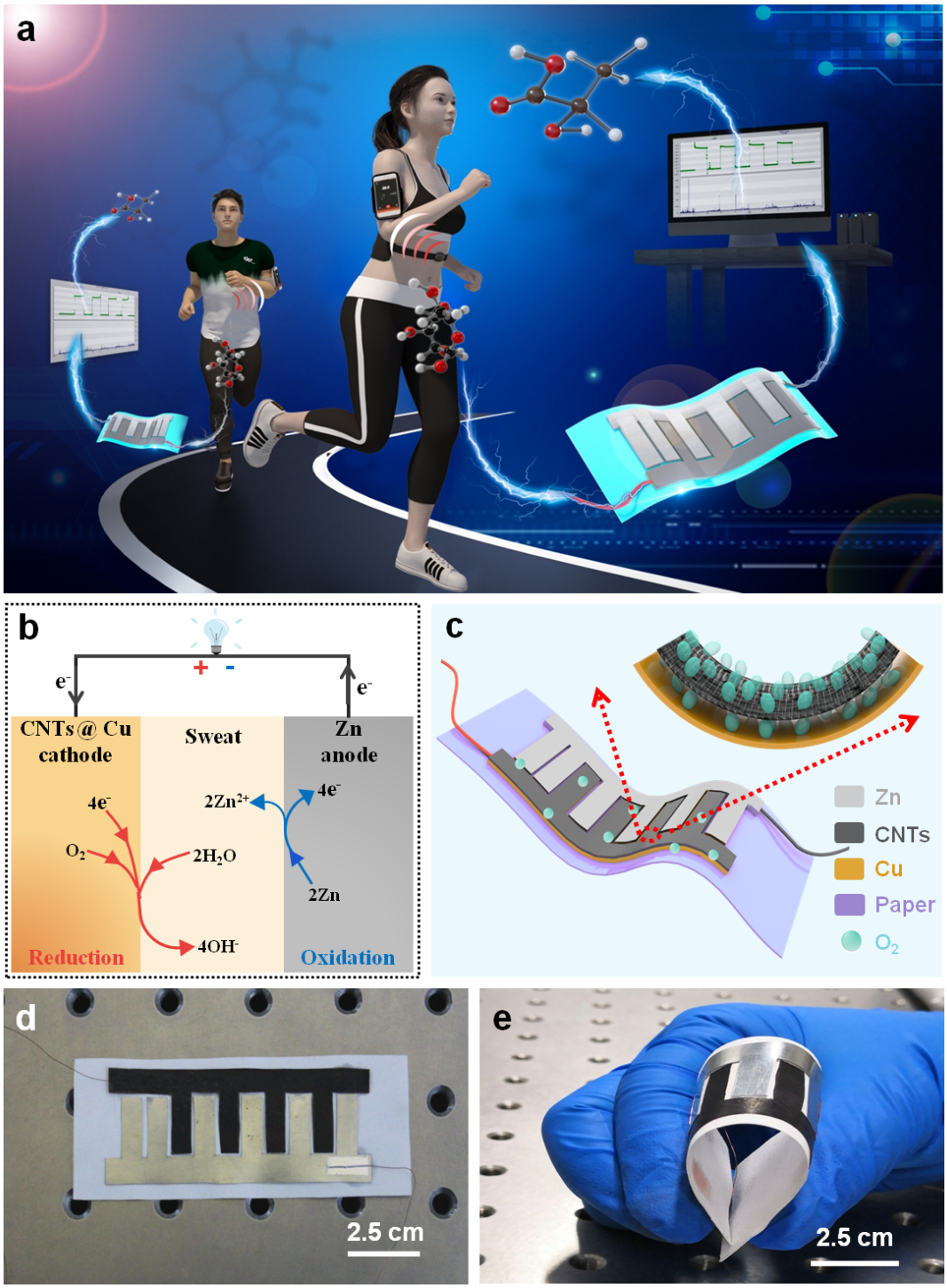

Figure 1. An overview of the SEG and its power generating mechanism. (**a**) Overview of the characterization and application of the SEG. (**b**) Schematic diagram of SEG's principle for electrochemical power generation. (**c**) Schematic diagram of the designed SEG. (**d**) Optical image of SEG after design optimization. (**e**) Optical image of a flexible SEG.

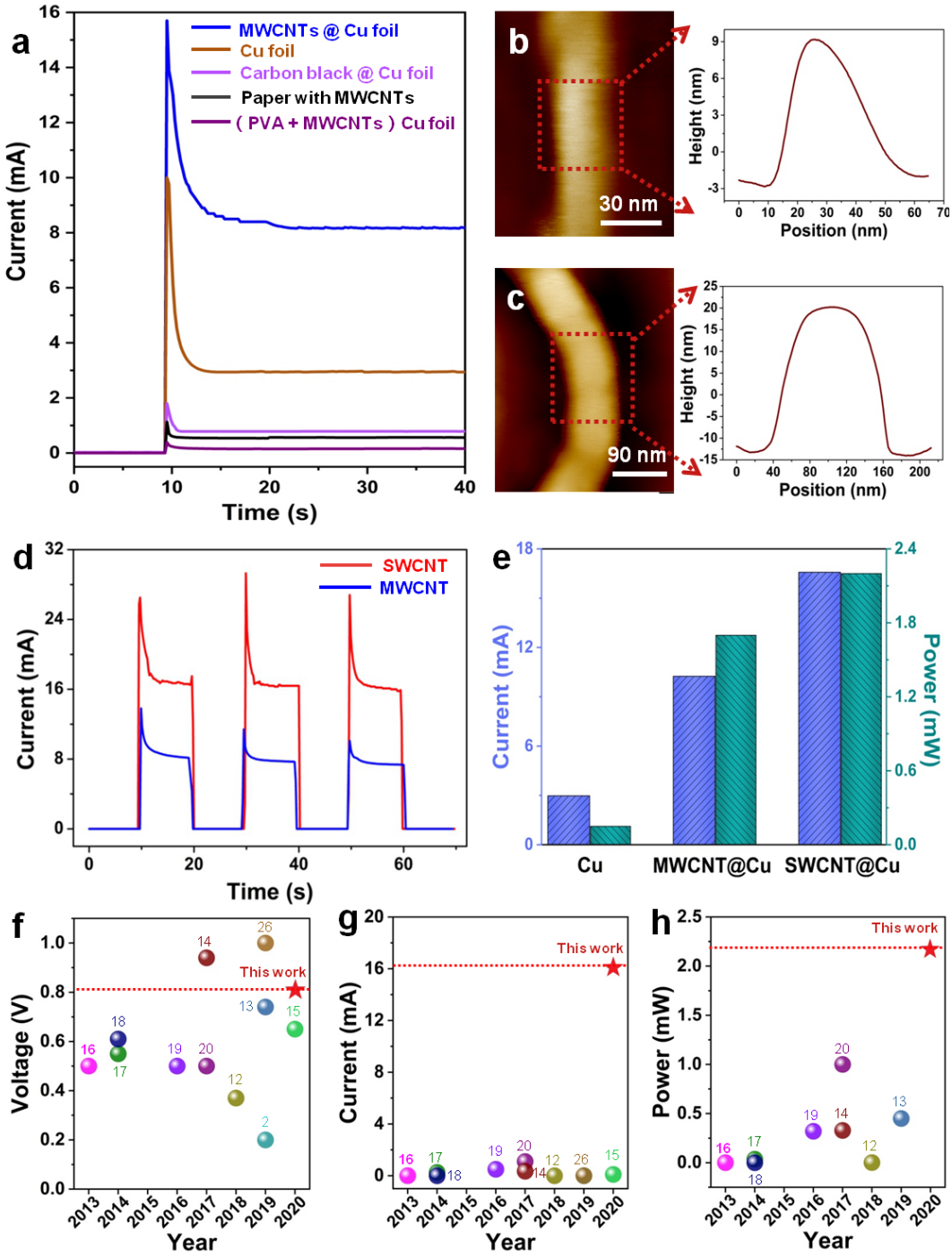

Figure 2. Optimization for output performance of SEG and comparison of device performance advantages. (**a**) Diagram of the output current of a SEG with a cathode coated with different carbon materials. (**b**) AFM characterization of a single SWCNT (illustrated in the position-height diagram of the selected region). (**c**) AFM representation of a single MWCNT (illustrated as a position-height diagram for the selected region). (**d**) Comparison of the output current between the SEG of SWCNT modified copper foil cathode and MWCNT modified copper foil cathode. (**e**) Histogram of output current and maximum power of a SEG with uncoated, MWCNT coating and SWCNT coating modified copper foil cathode. (**f-h**) Performance comparison of existing battery-free sweat devices (2,8,12-20,26).

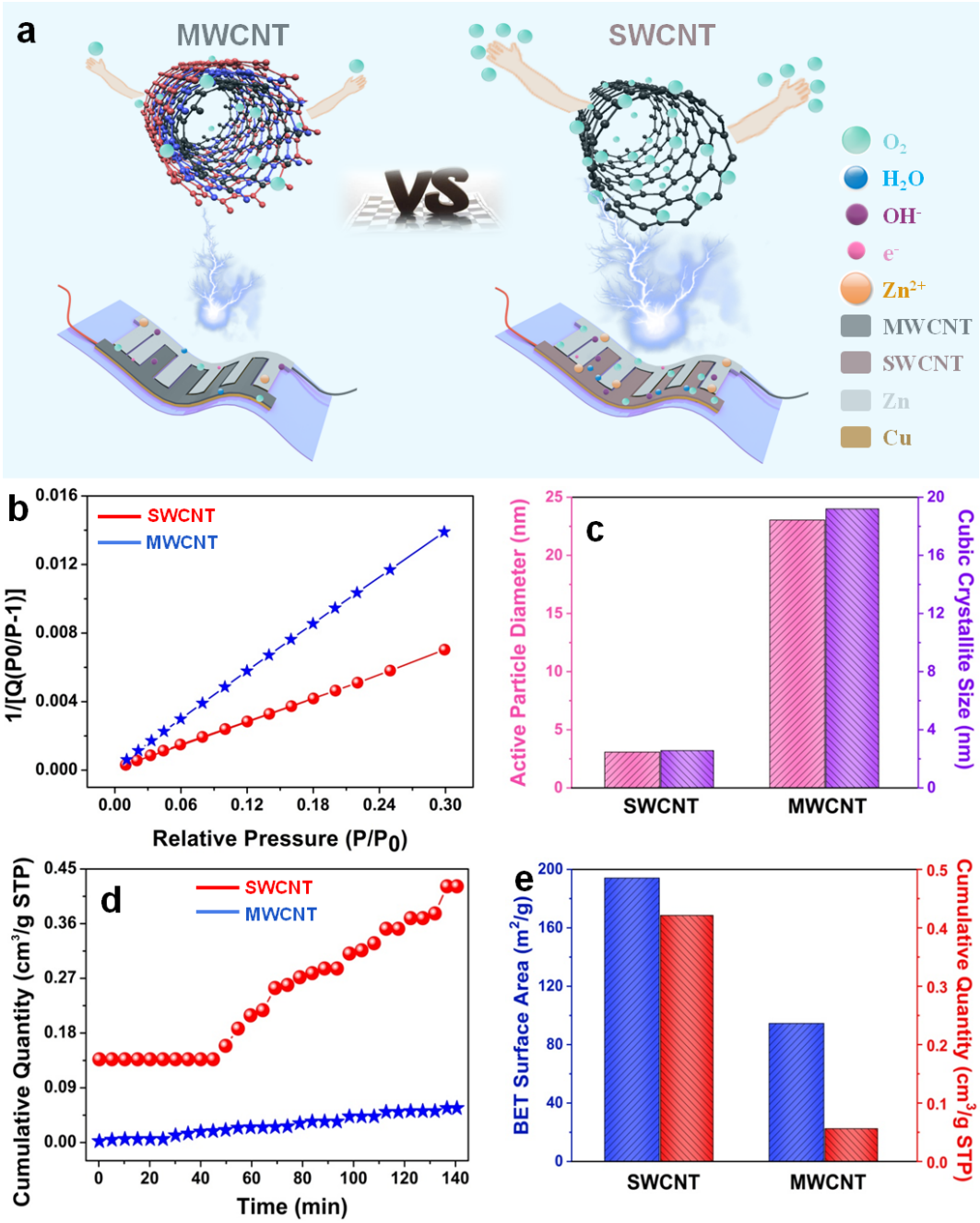

Figure 3. Study on the mechanism of CNTs in enhancing the output current of SEG. (**a**) Schematic of carbon nanotubes increasing the output current of a SEG. (**b**) BET surface area plot of SWCNTs and MWCNTs. (**c**) Histogram of active particle diameter and cubic crystallite of SWCNT and MWCNT samples. (**d**) Curves of oxygen quantity changing with time in SWCNT and MWCNT chemosorption within 140 min. (**e**) Histogram of the BET specific surface area and the cumulative quantity of chemisorption oxygen of SWCNT and MWCNT samples.

Table of Content graphic